JPEDAV (2007) 28:503–509
DOI: 10.1007/s11669-007-9199-2
1547-7037 ©ASM International

Ternary Diffusion in a RuAl-NiAl Couple

K.N. Kulkarni, B. Tryon, T.M. Pollock, and M.A. Dayananda

(Submitted January 19, 2007; in revised form June 22, 2007)

A ternary diffusion couple assembled with NiAl and RuAl disks and annealed at 1100 °C was examined by scanning electron microscopy and analyzed for concentration profiles by electron microprobe analysis. Complete mutual solid solubility with continuous variations in compositions was observed between the binary *B*2 aluminides. Ternary interdiffusion coefficients were determined with the aid of a program called *Multi*DiFlux over two composition ranges, one Ru-rich and the other Ni-rich, within the diffusion zone. The interdiffusion coefficient, $\tilde{\tilde{D}}^{Al}_{RuRu}$ varies little with variation in composition, but the interdiffusion coefficient, $\tilde{\tilde{D}}^{Al}_{NiNi}$ decreases by an order of magnitude from the Ni-rich region to the Ru-rich region. $\tilde{\tilde{D}}^{Al}_{NiNi}$ is larger than $\tilde{\tilde{D}}^{Al}_{RuRu}$ in the Ni-rich region by an order of magnitude. The cross coefficients, $\tilde{\tilde{D}}^{Al}_{NiRu}$ and $\tilde{\tilde{D}}^{Al}_{RuNi}$, are both positive. $\tilde{\tilde{D}}^{Al}_{NiRu}$ is comparable in magnitude to the main coefficient $\tilde{\tilde{D}}^{Al}_{NiNi}$ in the Ni-rich region; hence, Ni interdiffusion flux is enhanced down a Ru concentration gradient but decreased against it. Similarly, Ni interdiffusion is reduced down Al gradients. Characteristic depth parameters calculated for Ni and Ru are larger on the NiAl side than on the RuAl side. Approximate calculations of cumulative intrinsic diffusion fluxes past a Kirkendall plane suggest that the atomic mobility of Ni is larger than that of Ru.

Keywords modeling, nickel aluminide, ruthenium aluminide, ternary diffusion

1. Introduction

Ru additions to Ni-base superalloys and thermal barrier coating (TBC) systems have recently been investigated to increase the high-temperature capabilities of these systems.[1-7] Specifically for TBCs the system life may be prolonged if the creep resistance of NiAl-based bond coats is improved.[8,9] Thus, creep-resistant Ru-containing bond coats for thermal barrier coating systems are of interest, particularly since the creep strength of bulk RuAl has been shown to be substantially higher than that of bulk NiAl.[6]

The ternary Ru-Al-Ni system forms the basis of this study. Since NiAl and RuAl both have *B*2 crystal structures, phase equilibria and the possibility of a miscibility gap in the ternary system have been of interest.[10-17] Based on a recent experimental study of the Ru-Al-Ni ternary system at the temperatures of 1000 and 1100 °C,[17] the two *B*2 phases form a continuous solid solution. A Ru-Al-Ni isotherm at 1100 °C is shown in Fig. 1. The lattice parameters for the binary RuAl and NiAl phases are reported[18] to be 0.299 and 0.289 nm, respectively. Since the lattice mismatch between NiAl and RuAl is quite small, the variation in the molar volume of the ternary Ru-Al-Ni *B*2 phase is considered negligible.

To date, Ru interdiffusion has only been studied in dilute γ-Ni alloys.[19] There are no data on interdiffusion in ternary Ru-Al-Ni alloys. More comprehensive interdiffusion information about this ternary system is not only useful from a transport viewpoint, but is also important for understanding rate-limiting processes in high-temperature creep of Ru-containing NiAl materials. Interdiffusion coefficients for the Ru-Al-Ni ternary alloys are difficult to compute using the conventional Boltzmann-Matano method or numerical methods suggested by Sauer and Freise[20] or den Broeder,[21] since the description of interdiffusion in an *n*-component system requires the determination of $(n-1)^2$ interdiffusion coefficients.[22] New analytical models designed to calculate concentration-dependent interdiffusion coefficients in multicomponent alloys are useful for extracting this information.[23]

Experimental determination of ternary interdiffusion coefficients by the Boltzmann-Matano method requires two independent diffusion couples with intersecting diffusion paths.[24] An alternative method has been developed by Dayananda and Sohn[25-27] for the determination of interdiffusion coefficients in ternary systems with just one couple. Based on the Dayananda analysis, Dayananda and Ram-Mohan[28] have developed a user-friendly computer program called "*Multi*Diflux" for the analysis of *n*-component diffusion couples. This program determines the interdiffusion fluxes directly from the concentration profiles and calculates the $(n-1)^2$ interdiffusion coefficients over selected regions in the diffusion zone. The program also regenerates the concentration profiles using the Transfer Matrix Method (TMM) developed by Ram-Mohan and Dayananda.[29,30] Applications of the *Multi*Diflux program to analyze interdiffusion in ternary[23,31] and quaternary[32] systems have been

K.N. Kulkarni and **M.A. Dayananda,** School of Materials Engineering, Purdue University, West Lafayette, IN, USA; **B. Tryon** and **T.M. Pollock,** Department of Materials Science and Engineering, University of Michigan, Ann Arbor, MI, USA. Contact e-mail: dayanand@ecn.purdue.edu.

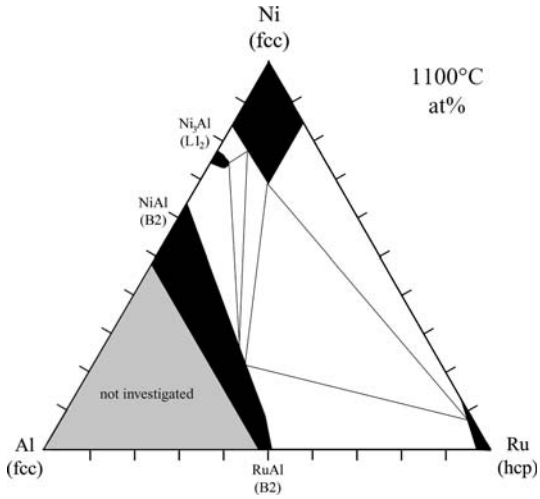

Fig. 1 Experimentally assessed Ru-Al-Ni ternary phase diagram at 1100 °C. Source: Ref 17

discussed elsewhere. In this paper average interdiffusion coefficients are determined with the aid of the *Multi*Diflux program for a Ru-Al-Ni ternary diffusion couple assembled with NiAl and RuAl alloys and annealed at 1100 °C. The couple is also analyzed for the cumulative intrinsic fluxes of Ru and Ni past a plane identified by Kirkendall pores in the diffusion zone. Diffusion depths of the individual elements on either side of the Matano plane are also reported in terms of characteristic depth parameters[33] evaluated from interdiffusion fluxes.

2. Experimental Procedure

Diffusion couples were formed by joining blocks of stoichiometric single-crystal NiAl with near-stoichiometric, arc melted RuAl in a vacuum furnace under a 20 MPa load for 24 h at 1000 °C. One couple in the "as-joined" condition was set aside for observation. Another couple was sealed in Ar-backfilled quartz tube and annealed for 336 h at 1100 °C. The couple was sectioned and prepared by traditional metallographic means and examined via scanning electron microscopy (SEM).

Concentration profiles across the diffusion-annealed couple were measured by electron probe microanalysis (EPMA) using stoichiometric NiAl and RuAl as standards for calibration. The RuAl and NiAl standards used for this analysis had been independently checked for composition in previous investigations by wavelength dispersive spectroscopy, x-ray diffraction, and transmission electron microscopy.[34] A CAMECA SX 100 electron probe microanalyzer (CAMECA S.A.S. 92403 Courbevoie Cedex, France; University of Michigan, Ann Arbor, Michigan) (with accelerating voltage and beam current set to 20 kV and 10 nA, respectively) was used to generate the concentration profiles. Ni Kα, Al Kα, and Ru Lα lines were used for the analysis of Ni, Al, and Ru, respectively. Count times for peak positions were set at 10 s, while each background position was counted for 5 s. Corrections to the EPMA measurements were made using CAMECA's PeakSight software, which uses a PAP model for the *Z* (atomic number), *A* (absorption), and *F* (fluorescence) correction employing an algorithm written by Pouchou and Pichoir.[35] Several line scans were taken across the couple with step sizes ranging from 2 to 10 μm. The electron interaction volume of the beam was determined to be 1 to 2 μm^3. The experimental concentration profiles are analyzed for the determination of the ternary interdiffusion coefficients and assessment of diffusional interactions among the components.

3. Analysis of Ternary Diffusion

3.1 The Basis of the MultiDiFlux Program

For the analysis of an isothermally annealed *n*-component diffusion couple, the *Multi*DiFlux program[28] employs cubic Hermite interpolation[36] for fitting the concentration profiles of the individual components. The fitted curves are then used for calculating the interdiffusion fluxes and the $(n-1)^2$ interdiffusion coefficients over selected regions in the diffusion zone. The interdiffusion flux $\tilde{J}_i$ of a component i at any section x is calculated directly from the fitted concentration profiles from:[26,27]

$$\tilde{J}_i = \frac{1}{2t} \int_{C_i^- \text{ or } C_i^+}^{C_i(x)} (x - x_0)\, dC_i \qquad (i = 1, 2, 3) \qquad \text{(Eq 1)}$$

where t is the diffusion time in seconds, C_i^- and C_i^+ are the terminal concentrations of component i, and x_0 is the location of the Matano plane. Here, the molar volume is assumed to be constant over the diffusion zone.

Onsager's formalism[37] of Fick's law extended to ternary systems is given by:

$$\tilde{J}_i = -\sum_{j=1}^{2} \tilde{D}_{ij}^{3} \frac{\partial C_j}{\partial x} \qquad (i = 1, 2) \qquad \text{(Eq 2)}$$

where $\tilde{D}_{ij}^{3}$ are the four concentration-dependent interdiffusion coefficients with the dependent component identified in the superscript as component 3. These coefficients are determined by the Dayananda analysis[25-27] as average values over selected composition ranges in the diffusion zone; they are identified by $\bar{\tilde{D}}_{ij}^{3}$ and are treated as constants over those composition ranges. In terms of the average interdiffusion coefficients, Eq 2 can be modified to:

$$\tilde{J}_i = -\sum_{j=1}^{2} \bar{\tilde{D}}_{ij}^{3} \frac{\partial C_j}{\partial x} \qquad (i = 1, 2) \qquad \text{(Eq 3)}$$

Multiplying both sides of Eq 3 by $(x - x_0)^p$ and integrating from x_1 to x_2 in the diffusion zone[25] we obtain

$$\int_{x_1}^{x_2} \tilde{J}_i (x - x_0)^p dx = -\sum_{j=1}^{2} \bar{\tilde{D}}_{ij}^{3} \int_{C_j(x_1)}^{C_j(x_2)} (x - x_0)^p dC_j \qquad (i = 1, 2) \qquad \text{(Eq 4)}$$

For p values of 0 and 1, Eq 4 yields four independent equations, which can be solved simultaneously for the four average interdiffusion coefficients for a ternary system. *Multi*Diflux evaluates the integrals involved in Eq 4 and solves for a set of four interdiffusion coefficients over any composition range or region selected within the diffusion zone. The number of regions and their selection are guided by the fact that the matrix of $\bar{\tilde{D}}^{3}_{ij}$ representing any selected region should be positive definite.[24] The program then uses the calculated $\bar{\tilde{D}}^{3}_{ij}$ to regenerate the concentration profiles over the selected composition ranges. For a ternary system, the regeneration of the concentration profiles is carried out[23,31] on the basis of error function solutions of Fujita and Gosting[38] or by employing the transfer matrix method (TMM) developed by Ram-Mohan and Dayananda.[29]

3.2 Determination of Characteristic Depth Parameters

For a relative measure of penetration depths of the individual components on either side of the Matano plane, characteristic depth parameters as defined by Dayananda[33] may be employed. On the left-hand side of the Matano plane a characteristic depth parameter $d_{i,\mathrm{L}}$ for component i is expressed by:

$$d_{i,\mathrm{L}} = \frac{\int_{-\infty}^{x_o} \tilde{J}_i(x)dx}{\tilde{J}_i(x_o)} \qquad \text{(Eq 5)}$$

and for the right-hand side of the Matano plane, the characteristic depth parameter $d_{i,\mathrm{R}}$ for component i is given by:

$$d_{i,R} = \frac{\int_{x_o}^{\infty} \tilde{J}_i(x)dx}{\tilde{J}_i(x_o)} \qquad \text{(Eq 6)}$$

4. Results and Discussion

A backscattered electron image of the NiAl/RuAl diffusion couple annealed at 1100 °C for 336 h is shown in Fig. 2. A change in contrast can be discerned across the interdiffusion region of the image due to difference in atomic masses of Ni and Ru. The experimental data on concentration profiles for the diffusion couple are presented in Fig. 3. The uncertainty in the measured concentration data was evaluated to be less than 1%. Also included in Fig. 3 are curves fitted to the experimental data with cubic Hermite polynomials by the *Multi*Diflux program. The composition profiles between the terminal RuAl and NiAl disks show the development of a ternary (Ru,Ni)Al region with continuous variations in the concentrations of all the components in the diffusion zone.

4.1 Determination of Ternary Interdiffusion Coefficients and Characteristic Depth Parameters

The analysis of a couple bonded at 1000 °C without further annealing indicated very little interdiffusion in the bond region. Thus, the limited interdiffusion that would have occurred during the bonding step has been ignored for the diffusion couple annealed at the higher temperature of 1100 °C for a longer time of 336 h. For the calculation of average ternary interdiffusion coefficients from the concentration profiles presented in Fig. 3, two adjacent regions, identified as region 1 and region 2, were selected. These regions are similar in width and cover different ranges of concentrations of Ni and Ru with small changes in the Al concentration.

The interdiffusion coefficients evaluated by the *Multi*DiFlux program are reported in Table 1 along with the concentration ranges of Ru, Ni, and Al for each region. Al is taken as the dependent variable in the calculation of the ternary interdiffusion coefficients. Uncertainties in the reported values of the average interdiffusion coefficients are estimated to be within 40%; they arise mainly from errors in the evaluation of the integrals involved in Eq 4 and depend on the relative magnitudes of the interdiffusion coefficients.

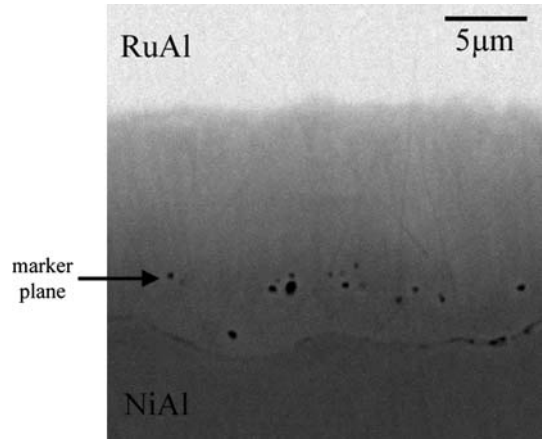

Fig. 2 Backscattered electron image of NiAl-RuAl diffusion couples annealed 336 h at 1100 °C

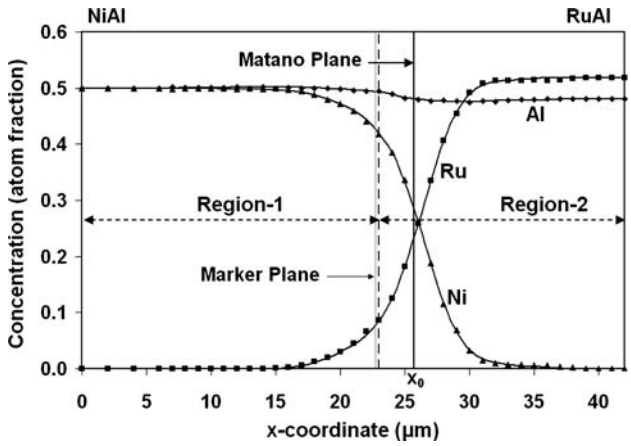

Fig. 3 Experimental data on concentration profiles fitted with Hermite interpolation polynomials for the NiAl-RuAl diffusion couple annealed at 1100 °C for 336 h

Table 1 Average interdiffusion coefficients evaluated over two different regions of the diffusion couple NiAl/RuAl annealed at 1100 °C for 336 h

Region	Range of *x*-coordinates	Range of composition, at.%			$\bar{\tilde{D}}_{ij}^{Al}$ (10^{-18} m^2/s)			
		Ru	Ni	Al	$\bar{\tilde{D}}_{RuRu}^{Al}$	$\bar{\tilde{D}}_{RuNi}^{Al}$	$\bar{\tilde{D}}_{NiRu}^{Al}$	$\bar{\tilde{D}}_{NiNi}^{Al}$
1	0-23	0-8.3	50-42.3	50-49.4	7.4	0.4	33.3	44.5
2	23-42	8.3-51.9	42.3-0	49.4-48.1	7.6	4.3	0.4	4.3

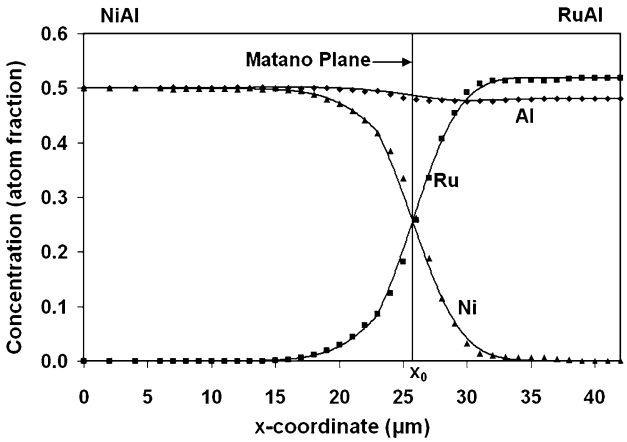

Fig. 4 Regenerated concentration profiles from the average interdiffusion coefficients reported in Table 1 for the diffusion couple NiAl-RuAl

The acceptability of the interdiffusion coefficients presented in Table 1 for the two regions is checked by regenerating the concentration profiles on the basis of error functions applicable to each region.[31] The regenerated concentration profiles for the couple are shown in Fig. 4; they represent the experimental profiles very well.

As indicated in Table 1, the Ru-concentration varies from 0 to 8.3 at.% in region 1 and from 8.3 to 51.9 at.% in region 2. Thus, region 1 is Ni-rich while region 2 is Ru-rich. As can be seen in Table 1, the main interdiffusion coefficient, $\bar{\tilde{D}}_{RuRu}^{Al}$, for Ru varies little from the Ni-rich region 1 to the Ru-rich region 2; on the other hand, the main interdiffusion coefficient, $\bar{\tilde{D}}_{NiNi}^{Al}$, for Ni decreases by an order of magnitude from region 1 to region 2. Also, $\bar{\tilde{D}}_{RuRu}^{Al}$ and $\bar{\tilde{D}}_{NiNi}^{Al}$ are of the same order of magnitude in the Ru-rich region but $\bar{\tilde{D}}_{NiNi}^{Al}$ is one order of magnitude greater than $\bar{\tilde{D}}_{RuRu}^{Al}$ in the Ni-rich region.

Regarding the cross interdiffusion coefficients, $\bar{\tilde{D}}_{NiRu}^{Al}$ is positive in both Ni-rich and Ru-rich regions. In addition, $\bar{\tilde{D}}_{NiRu}^{Al}$ is comparable in magnitude to the main coefficient of Ni, $\bar{\tilde{D}}_{NiNi}^{Al}$, in the Ni-rich region but is an order of magnitude smaller than $\bar{\tilde{D}}_{NiNi}^{Al}$ in the Ru-rich region. This observation implies that the interdiffusion flux of Ni increases down a Ru concentration gradient and decreases against it. Since $\bar{\tilde{D}}_{NiRu}^{Al}$ is equal to $-\bar{\tilde{D}}_{NiAl}^{Ru}$, $\bar{\tilde{D}}_{NiAl}^{Ru}$ is a negative number for the Ni-rich (Ru,Ni)Al alloys. Hence, Ni interdiffusion is decreased down an Al concentration gradient. Such diffusional interactions are stronger in the Ni-rich region than in the Ru-rich region. The negative values of the cross interdiffusion coefficients between Ni and Al are consistent with the diffusional interactions between Ni and Al reported by Sohn and Dayananda[39,40] in the Fe-Ni-Al *B*2 phase at 1000 °C and by Nesbitt and Heckel[41] in the Ni-Cr-Al face-centered cubic (fcc) phase at 1100 °C.

Similarly, $\bar{\tilde{D}}_{RuNi}^{Al}$ is positive in both regions; however, $\bar{\tilde{D}}_{RuNi}^{Al}$ is comparable in magnitude to the main coefficient $\bar{\tilde{D}}_{RuRu}^{Al}$ on the Ru-rich side. Thus, the interdiffusion flux of Ru is reduced against the concentration gradient of Ni, and this effect is quite strong on the Ru-rich side of the diffusion zone in Fig. 3.

The selection of the two regions for the calculation of average interdiffusion coefficients was guided by the following two requirements. The first one was that each selected region should include segments of concentration profiles exhibiting nonzero gradients for each component. The second requirement is that the solution of the four equations set up on the basis of Eq 4 for each region corresponds to a matrix of four average interdiffusion coefficients that is positive definite with real and positive eigenvalues. Provided these requirements are satisfied, small variations in the selected regions will yield average interdiffusion coefficients that exhibit similar variations from one region to another.

The average interdiffusion coefficients reported in Table 1 were determined with Al as the dependent component. These data may be compared with the binary interdiffusion data available for the Ru and Ni system.[19] Karunaratne and Reed[19] have reported the binary average interdiffusion coefficients for two couples Ni/Ni-5 wt%Ru and Ni/Ni-10 wt%Ru at 1100 °C. The average binary interdiffusion coefficients they reported are approximately 5 to 6.3×10^{-16} m^2/s. The main ternary coefficients for Ni and Ru determined in our study at 1100 °C (see Table 1) are one to two orders of magnitude smaller than the binary interdiffusion coefficients reported by Karunaratne and Reed.[19] Thus, the presence of Al slows down the interdiffusion of Ni and Ru at 1100 °C.

For the Ru-Al-Ni (*B*2) alloys, it has been observed that the melting temperature increases as the Ru/Ni ratio increases.[42] For example, an alloy with 5Ru-40Al-55Ni (at.%) melts at 1729 °C, while the alloy 45Ru-50Al-5Ni[42] melts at 1970 °C. This observation also suggests that the interdiffusion becomes sluggish with increase in the Ru content.

In Table 2 are presented characteristic depth parameters, $d_{i,L}$ and $d_{i,R}$, for the left side and right side of the Matano plane calculated for both Ru and Ni on the basis of Eq 5 and 6.

Table 2 Characteristic depth parameters on either side of the Matano plane for Ni and Ru

Component	$d_{i,L}$, μm	$d_{i,R}$, μm
Ru	4.8	3.4
Ni	5.3	3.9

The left and right sides of the Matano plane in Fig. 3 refer to NiAl and RuAl sides, respectively. The characteristic depth parameters for Ni are slightly larger than those for Ru in both the Ni-rich and Ru-rich regions of the diffusion couple. Also, the parameters for both Ni and Ru are larger on the Ni-rich side than on the Ru-rich side.

Note that the penetration depths of a component as defined by Eq 5 and 6 depend on the integrated interdiffusion coefficient $\tilde{D}^{\text{Int}}_{i,\Delta C}$ given by:

$$\tilde{D}^{\text{Int}}_{i,\Delta C} = \int_{x_1}^{x_2} \tilde{J}_i(x)dx$$

On the basis of Eq 2 and 4, $\tilde{D}^{\text{Int}}_{i,\Delta C}$ becomes:[33]

$$\tilde{D}^{\text{Int}}_{i,\Delta C} = \sum_{j=1}^{n-1} \overline{\tilde{D}^{n}_{ij}}[C_j(x_1) - C_j(x_2)]$$

Thus, the diffusion depths depend on both the main and cross interdiffusion coefficient for a component as well as on the concentration differences of the individual components. The calculated values of the $\tilde{D}^{\text{Int}}_{i,\Delta C}$ are found to be similar in magnitude for Ni and Ru on both sides of the Matano plane. These values expressed in atomic fraction $\mu m^2/s$ for Ni and Ru, respectively, are 1.34×10^{-6} and -1.23×10^{-6} on the left side on of the Matano plane and 9.89×10^{-7} and -8.7×10^{-7} on the right side of the Matano plane in Fig. 3.

4.2 Intrinsic Diffusion

In the backscattered electron image presented in Fig. 2 can be seen a line of Kirkendall pores developed on the NiAl side of the couple. The line of pores may be identified with a marker plane x_m for an approximate estimation of the cumulative intrinsic fluxes of the individual components. If the marker plane moves parabolically with time at a constant composition, the cumulative or total intrinsic flux A_i of component i past the marker plane over the diffusion time t is defined by:

$$A_i = \int_0^t J_i dt \qquad \text{(Eq 7)}$$

where J_i refers to the intrinsic diffusion flux at the marker plane. A_i can be calculated on the basis of Heumann's method[43] from appropriate areas under the concentration profiles. Such areas, A_{Ru} and A_{Ni}, for Ru and Ni are shown as hatched areas in Fig. 5, where x_m denotes the location of the marker plane identified at the approximate composition 7.4Ru-43Ni-49.6Al. Magnitudes of A_{Ru} and A_{Ni} are,

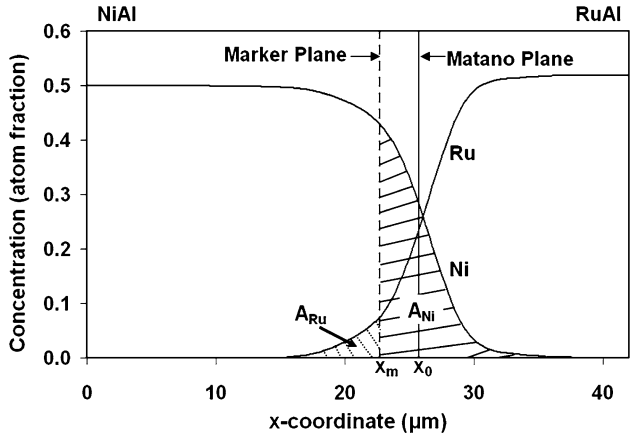

Fig. 5 Cumulative intrinsic diffusion fluxes of Ni and Ru past a marker plane are determined by areas, A_{Ni} and A_{Ru}; the marker plane corresponds to a line of pores observed in the diffusion zone of the NiAl-RuAl diffusion couple

respectively, 0.18 and 1.8 atomic fraction μm; thus, A_{Ni} is about 10 times larger than A_{Ru} in magnitude. Based on a simple atomic mobility model it can be shown[44] that

$$A_i = -2tC_i\beta_i\left(\frac{\partial\mu_i}{\partial x}\right)_{x_m} \qquad \text{(Eq 8)}$$

where β_i and μ_i refer to the atomic mobility and chemical potential of component i. C_{Ni} is more than five times larger than C_{Ru} at x_m in Fig. 5. The calculation of mobilities from Eq 8 requires thermodynamic information for (Ni,Ru)Al alloys. If the chemical potential gradients of Ni and Ru at x_m are similar in magnitude, β_{Ni} is expected to be larger than β_{Ru}.

From Fig. 3 it can be seen that the aluminum concentrations of the terminal aluminides of the diffusion couple remain similar. Hence, the interdiffusion fluxes of Al are quite small throughout the diffusion zone. Calculations of the characteristic depth parameters and cumulative intrinsic diffusion fluxes of Al suffer from large errors and are not reported.

5. Conclusions

A ternary diffusion couple assembled with NiAl and RuAl disks and annealed at 1100 °C showed complete mutual solid solubility with continuous variations in compositions between the terminal disks. From an analysis of the concentration profiles with the aid of the *Multi*DiFlux program, ternary interdiffusion coefficients were determined over two adjacent composition ranges, one Ru-rich and the other Ni-rich, in the diffusion zone. The main interdiffusion coefficient, $\bar{\tilde{D}}^{\text{Al}}_{\text{RuRu}}$, for Ru is similar for both regions, while the main interdiffusion coefficient, $\bar{\tilde{D}}^{\text{Al}}_{\text{NiNi}}$, for Ni decreases by an order of magnitude from the Ni-rich region to the Ru-rich region. $\bar{\tilde{D}}^{\text{Al}}_{\text{NiNi}}$ is an order of magnitude larger than $\bar{\tilde{D}}^{\text{Al}}_{\text{RuRu}}$ in the Ni-rich region. The cross coefficients $\bar{\tilde{D}}^{\text{Al}}_{\text{NiRu}}$ and $\bar{\tilde{D}}^{\text{Al}}_{\text{RuNi}}$ are both positive, and $\bar{\tilde{D}}^{\text{Al}}_{\text{NiRu}}$ is comparable to the main

coefficient $\tilde{\tilde{D}}^{Al}_{NiNi}$ in the Ni-rich region. The interdiffusion flux of Ni is increased down a Ru concentration gradient. Alternatively, interdiffusion of Ni in the ternary (Ru,Ni)Al alloys is reduced down Al concentration gradients. Characteristic depth parameters calculated for both Ni and Ru are larger on the NiAl side than on the RuAl side. Approximate calculations of the cumulative intrinsic diffusion fluxes across a Kirkendall plane of pores suggest that the atomic mobility of Ni is larger than that of Ru.

Acknowledgments

Research supported by a program of international collaboration between the National Science Foundation (DMR-0099695) and the European Commission (GRD2-200-30211). Single crystal bars of NiAl were provided by R. Darolia of the General Electric Corporation. The *Multi*DiFlux program employed for the analysis of the diffusion couple for ternary interdiffusion coefficients was developed at Purdue University under the NSF grant DMR 0304777.

References

1. Q. Feng, T.K. Nandy, S. Tin, and T. Pollock, Solidification of High Refractory Ruthenium-Containing Superalloys, *Acta Mater.*, 2003, **51**(1), p 269-284
2. Q. Feng, T.K. Nandy, and T. Pollock, Observation of a Ruthenium-Rich Heusler Phase in Ruthenium-Containing Superalloys, *Scr. Mater.*, 2004, **50**(6), p 849-854
3. Q. Feng, T.K. Nandy, and T.M. Pollock, The Re (Ru)-rich δ-phase in Ru-containing superalloys, *Mater. Sci. Eng. A*, 2004, **373**(1-2), p 239-249
4. Q. Feng, T.K. Nandy, L.J. Rowland, B. Tryon, D. Banerjee, and T.M. Pollock, New Phases in Ruthenium-Containing Single-Crystal Superalloys, in *Superalloys 2004: The Tenth International Symposium on Superalloys*, The Minerals, Metals, & Materials Society, Seven Springs, PA, 2004, p 769-778
5. B. Tryon, Q. Feng, and T. Pollock, Intermetallic Phases Formed by Ruthenium-Nickel Alloy Interdiffusion, *Intermetallics*, 2004, **12**(7-9), p 957-962
6. B. Tryon, F. Cao, K.S. Murphy, C.G. Levi, and T.M. Pollock, Ruthenium-Containing Bond Coats for Thermal Barrier Coating Systems, *J. Met.*, 2006, **58**(1), p 53-59
7. B. Tryon, Q. Feng, R.W. Wellman, K.S. Murphy, J. Yang, C.G. Levi, J.R. Nicholls, and T.M. Pollock, Multi-layered Ruthenium-Containing Bond Coats for Thermal Barrier Coatings, *Metall. Mater. Trans. A*, 2006, **37A**(11), p 3347-3358
8. A.M. Karlsson and A.G. Evans, A Numerical Model for the Cyclic Instability of Thermally Grown Oxides in Thermal Barrier Systems, *Acta Mater.*, 2001, **49**(10), p 1793-1804
9. D.S. Balint and J.W. Hutchinson, Undulation Instability of a Compressed Elastic Film on a Nonlinear Creeping Substrate, *Acta Mater.*, 2003, **51**(13), p 3965-3983
10. S. Chakravorty and D.R.F. West, Phase Equilibria Between NiAl and RuAl in the Ni-Al-Ru System, *Scr. Metall.*, 1985, **19**(11), p 1355-1360
11. S. Chakravorty and D.R.F. West, The Constitution of the Ni-Al-Ru System, *J. Mater. Sci.*, 1986, **21**, p 2721-2730
12. I.J. Horner, L.A. Cornish, and M.J. Witcomb, A Study of the Al-Ni-Ru Ternary System Below 50 at.% Aluminium, *J. Alloys Compd.*, 1997, **256**(1-2), p 213-220
13. I.J. Horner, L.A. Cornish, and M.J. Witcomb, Constitution of the Al-Ni-Ru Ternary System Above 50 at.% Aluminium, *J. Alloys Compd.*, 1997, **256**(1-2), p 221-227
14. I.J. Horner, N. Hall, L.A. Cornish, M.J. Witcomb, M.B. Cortie, and T.D. Boniface, An Investigation of the B2 Phase Between AlRu and AlNi in the Al-Ni-Ru Ternary System, *J. Alloys Compd.*, 1998, **264**(1-2), p 173-179
15. P. Gargano, H. Mosca, G. Bozzolo, and R.D. Noebe, Atomistic Modeling of RuAl and (RuNi)Al Alloys, *Scr. Mater.*, 2003, **48**(6), p 695-700
16. I. Vjunitsky, E. Schönfeld, T. Kaiser, W. Steurer, and V. Shklover, Study of Phase States and Oxidation of B2-Structure Based Al-Ni-Ru-M Alloys, *Intermetallics*, 2005, **13**(1), p 35-45
17. B. Tryon and T.M. Pollock, Experimental Assessment of the Ru-Al-Ni Ternary Phase Diagram at 1000 and 1100 °C, *Mater. Sci. Eng. A*, 2006, **430**(1-2), p 266-276
18. I.M. Wolff, G. Sauthoff, L.A. Cornish, H.D. Steyn, and R. Coetzee, Structure-Property-Application Relationships In Ruthenium Aluminide RuAl, *Proceedings of Second International Conference on Structural Intermetallics*, TMS publication, 1997, p 815-823
19. M.S.A. Karunaratne and R.C. Reed, Interdiffusion of the Platinum-Group Metals in Nickel at Elevated Temperatures, *Acta Mater.*, 2003, **51**(10), p 2905-2919
20. F. Sauer and V. Freise, *Z. Elektrochem*, 1962, **66**, p 353-363
21. F.J.A. den Broeder, A General Simplification and Improvement of the Matano-Boltzmann Method in the Determination of the Interdiffusion Coefficients in Binary Systems, *Scr. Metall.*, 1969, **3**(5), p 321-325
22. M.E. Glicksman, *Diffusion in Solids*. John Wiley & Sons, New York, 2000
23. K.M. Day, L.R. Ram-Mohan, and M.A. Dayananda, Determination and Assessment of Ternary Interdiffusion Coefficients from Individual Diffusion Couples, *J. Phase Equilib. Diffus.*, 2005, **26**(6), p 579-590
24. J.S. Kirkaldy and D.J. Young, *Diffusion in the Condensed State*. The Institute of Metals, London, 1987
25. M.A. Dayananda and Y.H. Sohn, A New Analysis for the Determination of Ternary Interdiffusion coefficients from a Single Diffusion Couple, *Metall. Mater. Trans. A*, 1999, **30A**(3), p 535-543
26. M.A. Dayananda and C.W. Kim, Zero-Flux Planes and Flux Reversals in Cu-Ni-Zn Diffusion Couples, *Metall. Trans. A*, 1979, **10**(9), p 1333-1339
27. M.A. Dayananda, An Analysis of Concentration Profiles for Fluxes, Diffusion Depths, and Zero-Flux Planes in Multicomponent Diffusion, *Metall. Trans. A*, 1983, **14**(9), p 1851-1858
28. M.A. Dayanand and L.R. Ram-Mohan, *MultiDiflux*, Purdue University, 2005, https://engineering.purdue.edu/MSE/Fac_-Staff/dayanand.wshtml
29. L.R. Ram-Mohan and M.A. Dayananda, A Transfer Matrix Method for the Calculation of Concentrations and Fluxes in Multicomponent Diffusion Couples, *Acta Mater.*, 2006, **54**(9), p 2325-2334
30. L.R. Ram-Mohan and M.A. Dayananda, A Transfer-Matrix Method for Analysis of Multicomponent Diffusion with any Number of Components, *J. Phase Equilib. Diffus.*, 2006, **27**(6), p 566-571
31. M.A. Dayananda, Analysis of Multicomponent Diffusion Couples for Interdiffusion Fluxes and Interdiffusion Coefficients, *J. Phase Equilib. Diffus.*, 2005, **26**(5), p 441-446
32. K.N. Kulkarni, A.M. Girgis, L.R. Ram-Mohan, and M.A. Dayanand, A Transfer Matrix Analysis of Quaternary Diffusion, *Philos. Mag.*, 2007, **87**(6), p 853-872

33. M.A. Dayananda, Average Effective Interdiffusion Coefficients and the Matano Plane Composition, *Metall. Mater. Trans. A*, 1996, **27**(9), p 2504-2509
34. T.M. Pollock, D.C. Lu, X. Shi, and K. Eow, A Comparative Analysis of Low Temperature Deformation in B2 Aluminides, *Mater. Sci. Eng. A*, 2001, **317**(1-2), p 241-248
35. J.L. Pouchou and F. Pichoir, A New Model for Quantitative X-Ray-Microanalysis. 1.Application to the Analysis of Homogeneous Samples, *Recherche Aerospatiale*, 1984, **3**, p 13-18, English Edition
36. L.R. Ram-Mohan, *Finite Element and Boundary Element Applications to Quantum Mechanics*. Oxford University Press, Oxford, UK, 2002, p 63-81
37. L. Onsager, Reciprocal Relations in Irreversible Processes. I, *Phys. Rev.*, 1931, **37**(4), p 405-426
38. H. Fujita and L.J. Gosting, An Exact Solution of the Equations for Free Diffusion in 3-Component Systems with Interacting Flows, and Its Use in Evaluation of the Diffusion Coefficients, *J. Am. Chem. Soc.*, 1956, **78**(6), p 1099-1106
39. Y.H. Sohn and M.A. Dayananda, Diffusion Studies in the (B2), (BCC), and (FCC) Fe-Ni-Al Alloys at 1000°C, *Metall. Mater. Trans. A*, 2002, **33A**(11), p 3375-3392
40. Y.H. Sohn and M.A. Dayananda, A Double-Serpentine Diffusion Path for a Ternary Diffusion Couple, *Acta Mater.*, 2000, **48**(7), p 1427-1433
41. J.A. Nesbitt and R.W. Heckel, Interdiffusion in Ni-Rich, Ni-Cr-Al Alloys at 1100°C and 1200°C. 2. Diffusion-Coefficients and Predicted Concentration Profiles, *Metall. Trans. A*, 1987, **18**(12), p 2075-2086
42. F. Cao., PhD Thesis, University of Michigan, 2006
43. T. Heumann, *Z. Physik. Chem.*, 1952, **201**, p 168
44. M.A. Dayanand, Atomic Mobilities in Multicomponent Diffusion and Their Determination, *Trans. Metall. Soc. AIME*, 1968, **242**(7), p 1369-1370